J Physiol 590.11 (2012) pp 2645–2657

The Journal of Physiology

Kv1.1-dependent control of hippocampal neuron number as revealed by mosaic analysis with double markers

Shi-Bing Yang[1], Kellan D. Mclemore[1,3], Bosiljka Tasic[2,4], Liqun Luo[2], Yuh Nung Jan[1] and Lily Yeh Jan[1]

[1]*Howard Hughes Medical Institute, Departments of Physiology, Biochemistry and Biophysics, University of California–San Francisco, San Francisco, CA, USA*
[2]*Department of Biology, Howard Hughes Medical Institute, Stanford University, Stanford, CA, USA*
[3]*Carleton College, Northfield, MN, USA*
[4]*Allen Institute for Brain Science, Seattle, WA, USA*

Key points

- The classical function of potassium channels in electrical signaling is to regulate nerve conduction, muscle contraction and hormone secretion.
- Certain types of potassium channels are also involved in regulating cell proliferation, as in the case of Kv1.1 mutant mice, which exhibit overgrowth of neurons and astrocytes thus leading to the phenotype of megencephaly, or enlarged brain, particularly in the hippocampus.
- We used a novel mouse genetic tool, Mosaic Analysis with Double Markers (MADM), to test whether Kv1.1 function is required cell-autonomously for megencephaly. We found that in the adult hippocampus, neurons but not astrocytes lacking Kv1.1 are more numerous than their counterparts with two functional alleles of Kv1.1.
- Our study reveals that loss of Kv1.1 function causes an overproduction of hippocampal neurons in a cell-autonomous manner.
- This study raises the prospect that targeting Kv1.1 potassium channel may help to induce neuron production.

Abstract *Megencephaly*, or *mceph*, is a spontaneous frame-shift mutation of the mouse Kv1.1 gene. This *mceph* mutation results in a truncated Kv1.1 channel α-subunit without the channel pore domain or the voltage sensor. Interestingly, *mceph*/*mceph* mouse brains are enlarged and – unlike wild-type mouse brains – they keep growing throughout adulthood, especially in the hippocampus and ventral cortex. We used mosaic analysis with double markers (MADM) to identify the underlying mechanism. In *mceph*-MADM6 mice with only a small fraction of neurons homozygous for the *mceph* mutation, those homozygous *mceph*/*mceph* neurons in the hippocampus are more abundant than wild-type neurons produced by sister neural progenitors. In contrast, neither *mceph*/*mceph* astrocytes, nor neurons in the adjacent dorsal cortex (including the entorhinal and parietal cortex) exhibited overgrowth in the adult brain. The sizes of *mceph*/*mceph* hippocampal neurons were comparable to *mceph*/+ or wild-type neurons. Our mosaic analysis reveals that loss of Kv1.1 function causes an overproduction of hippocampal neurons, leading to an enlarged brain phenotype.

(Received 18 January 2012; accepted after revision 6 March 2012; first published online 12 March 2012)
Corresponding author L. Y. Jan: Howard Hughes Medical Institute, Departments of Physiology, Biochemistry and Biophysics, University of California–San Francisco, San Francisco, CA, USA. Email: lily.jan@ucsf.edu

Abbreviations MADM, mosaic analysis with double markers.

DOI: 10.1113/jphysiol.2012.228486

Introduction

More than a century ago, the German physiologist Julius Bernstein proposed that potassium channels are the fundamental ionic conductances which determine the membrane potential in neurons (Bernstein, 1902). In their seminal paper six decades ago, Hodgkin and Huxley proposed that potassium channels set the resting potential and drive the repolarization and hyperpolarization phase of an action potential (Hodgkin & Huxley, 1952*b*). With the advance of molecular cloning, genetics and biophysical instrumental breakthrough, the biological functions of potassium channels uncovered include not only the orchestration of electrical activity in excitable tissues such as neurons and muscles but also the control of vital physiological functions including hormone secretion in pancreatic cells and electrolyte transport in kidney tubules (Shieh *et al.* 2000). Since the cloning of the *Drosophila Shaker* potassium channel gene (Papazian *et al.* 1987), more than 200 genes encoding various potassium channels have been characterized. The molecular architecture of a typical potassium channel is composed of four α-subunits, the main pore-forming protein, and several accessory β-subunits that often modify channel gating and trafficking properties of the α-subunits (Stühmer *et al.* 1989). Potassium channels have a pore structure well suited for efficient potassium flow close to the free diffusion limit ($\sim 10^8$ ions s^{-1}) as well as high selectivity to potassium over other cations such as sodium and calcium (Zhou & MacKinnon, 2003).

Voltage-gated potassium channels (Kv) are diverse (Jan & Jan, 1997). Hodgkin and Huxley formulated a simple yet elegant operating model for Kv channels to describe gating properties such as activation, inactivation and deactivation (Hodgkin & Huxley, 1952*a*). There are 12 voltage-gated potassium channel families (Kv1 to Kv12) with a range of channel properties (Gutman *et al.* 2005). The first four transmembrane segments of the α-subunits form the voltage sensing domain and control the gate of the pore formed by the pore loop and the flanking fifth and sixth transmembrane segments (Long *et al.* 2007). Kv channels are either homotetrameric or heterotetrameric; the N-terminal T1 domain is the molecular barcode for potassium channel tetramerization within each family (Covarrubias *et al.* 1991; Li *et al.* 1992; Sheng *et al.* 1992). Kv1 channels are highly expressed in the central nervous system and cardiovascular system, and in the nervous system, Kv1 channels are mainly located at axons and nerve terminals of a nerve cell (Wang *et al.* 1994; Campomanes *et al.* 2002), while some dendritic Kv1 channels are regulated by local activity and provide feedback regulation to its excitability (Shen *et al.* 2004; Guan *et al.* 2006). Physiological studies have also revealed that the Kv1 channels control action potential propagation and repolarization, set the resting membrane potential and modulate neurotransmitter release from nerve terminals (Glazebrook *et al.* 2002; Heeroma *et al.* 2009). Functions other than regulation of excitability have been suggested for different members of the Kv1 family, for Kv1.1 and Kv1.2 in the modulation of neuronal myelination by oligodendrocytes (Herrero-Herranz *et al.* 2007), and for Kv1.3, Kv1.4 and Kv1.5 in the control of glial cell function and glial precursor cell division (Preussat *et al.* 2003).

Thus, other than its well-known role in controlling cell excitability, potassium channels also control cell proliferation possibly by regulating membrane potentials that indirectly manipulate intracellular calcium, potassium and chloride, vital ions which regulate cell proliferation by controlling intracellular signalling or cell volume (Wonderlin & Strobl, 1996; Pardo, 2004). Interestingly, a recessive mutant *megencephaly* (*mceph*), so named for the phenotype of an enlarged brain, has arisen spontaneously (Donahue *et al.* 1996). Positional cloning revealed that this *mceph* mutant results from a deletion of 11 nucleotides in the Kv1.1 gene, the Shaker-like voltage-gated potassium channel in mouse, and this deletion leads to a frame-shift resulting in a truncation of Kv1.1 to include only the N-terminus and the first transmembrane segment (Petersson *et al.* 2003). Since the pore region (formed by the P-loop and the flanking 5th and 6th transmembrane segments) is missing, this MCEPH protein cannot form functional channel by itself or when it is co-assembled with other Kv1 channel α-subunits. However, since this truncated version of Kv1.1 contains the N-terminal T1 domain, an *in vitro* study has revealed that the MCEPH protein still can co-assemble with other α-subunits in the Kv1 channel family and suppresses Kv1 channel activity (Persson *et al.* 2005). The brain of the homozygous *mceph* mutant is significantly larger than wild-type brain starting from 3 weeks of age (Donahue *et al.* 1996). However, the *mceph*/*mceph* brain is not uniformly expanded: the hippocampus and ventral cortex are significantly increased in volume while other parts of the brain structure such as the adjacent dorsal cortex (including the entorhinal and parietal cortex), cerebellum and midbrain are comparable in size to the wild-type brain regions (Diez *et al.* 2003). Stereological and histological analysis has suggested that hyperplasia rather than hypertrophy causes this phenotype since the enlarged *mceph* hippocampus and ventral cortex contain more neurons and glial cells but the individual cell size is not abnormally large (Almgren *et al.* 2007). Indeed, the *mceph*/*mceph* brains continue to grow throughout adulthood, unlike wild-type brains that stop growing soon after birth. Previous studies have proposed multiple mechanisms to account for this megencephalic phenotype, including non-cell autonomous mechanisms such as an elevated level of trophic factors like the brain-derived neurotrophic factor (BDNF) (Lavebratt *et al.* 2006) and

cell-autonomous mechanisms such as reduced apoptosis and increased survival (Almgren *et al.* 2007).

We used a novel mouse genetic tool, mosaic analysis with double markers (MADM), to resolve cell-autonomous *versus* non-cell autonomous mecha nisms for the megencephalic phenotypes due to an over-abundance of neurons and glial cells. We found many more neurons homozygous for the *mceph* mutation in the hippocampus, especially in the dentate gyrus, a region with neurogenesis from embryogenesis to adulthood in mammals, but not in the adjacent dorsal cortex (including the entorhinal and parietal cortex), indicating the *mceph* mutation increases neuron number in a cell-autonomous fashion. Moreover, glial cells homozygous for the *mceph* mutation did not show any increase in number, indicating the increased gliogenesis in the *mceph*/*mceph* brain is caused by a non-cell-autonomous mechanism.

Methods

Animals

This study was carried out in strict accordance with the recommendations in the *Guide for the Care and Use of Laboratory Animals* of the National Institutes of Health, and used protocols approved by the Institutional Animal Care and Use Committee of the University of California–San Francisco. Both female and male mice were used for experiments and those mice were fed with chow diet and subjected to a 12/12 h day–night cycle. *mceph* and Nestin-cre mice were obtained from The Jackson Laboratory (Bar Harbor, ME, USA) and MADM6-GT and MADM6-TG mice were generated as described (Tasic *et al.* submitted). All mice were crossed to CD1 strain (Charles River, MA, USA) and maintained in the mixed genetic background.

Immunostaining

Mice, which were fed *ad libitum*, were anaesthetized by intraperitoneal Avertin injection and perfused transcardially with saline followed by 4% paraformaldehyde. Brains were removed and post-fixed overnight in 4% paraformaldehyde. Brains were then cryoprotected overnight in saline containing 30% sucrose at 4°C until they sank. Brain sections (50 μm) were washed in blocking medium containing 0.1% Triton X-100 and 5% donkey serum (Jackson ImmunoResearch Laboratories, Inc., West Grove, PA, USA), and incubated overnight (4°C) with primary antibodies against green fluorescent protein (GFP) (chicken 1:200, Aves, Tigard, OR, USA) c-myc (rabbit 1:200, Novus, Littleton, CO, USA), NeuN (rabbit, 1:400, Millipore, Billerica, MA, USA) and glial fibrillary acidic protein (GFAP) (rabbit, 1:400, Sigma-Aldrich, St Louis, MO, USA) followed by Alexa dye-tagged secondary antibodies (donkey 1:500, Invitrogen, Carlsbad, OR, USA). The slides were mounted using Fluoromount G mounting medium containing DAPI (Southern Biotech, Birmingham, AL, USA) and images were acquired using a confocal microscope (Zeiss, Germany).

Statistical analysis

We counted all the fluorescent neurons within the region of interest (such as the hippocampus or the adjacent dorsal cortex (including the entorhinal and parietal cortex) and quantified the percentage of red (*mceph*/*mceph*), green (wild-type Kv1.1) or yellow (*mceph*/+) in all fluorescent (red + green + yellow) neurons or astrocytes. Statistical analyses were performed with Prism software (GraphPad Software Inc., La Jolla, CA, USA) using Student's *t* test for pair-wise comparisons. $P < 0.05$ was considered statistically significant. The soma volume was measured using Zeiss LSM Image Browser and Imaris (Bitplane, South Windsor, CT, USA).

Results

Paradigm of generating mceph-MADM6 mice

We generated *mceph*-MADM6 mice to study the cell-autonomous and non-cell-autonomous mechanisms for the megencephalic phenotype (Fig. 1) (Zong *et al.* 2005; Tasic *et al.* submitted). In heterozygous *mceph*/+ mice with cre-recombinase active during the proliferative phase, somatic recombination may cause homozygosity of the *mceph* mutation distal to the MADM locus so that cells are marked with different colours according to their respective genotypes. Because homozygous mutant and homozygous wild-type cells are simultaneously generated as siblings and their progeny are labelled with different colours, the MADM mice have built-in control cells within the same brain region for phenotypic analysis (Espinosa *et al.* 2009; Liu *et al.* 2011). The mouse Kv1.1 gene is located about 8.8 centimorgan distal to the ROSA26 locus on chromosome 6 where the MADM gene cassette has been introduced (Petersson *et al.* 2003; Zong *et al.* 2005; Tasic *et al.* submitted). To generate homozygous *mceph*/*mceph* neurons throughout the entire nervous system in the *mceph*/+ genetic background, we crossed *mceph*/+;MADM6-TG/TG (MADM6-tdTomato (loxP)GFP) mice to nestin-cre;MADM6-GT/GT mice (MADM6-GFP(loxP)tdTomato). We chose the nestin-cre recombindase to induce interchromosomal recombination because nestin is an intermediate filament protein in the precursor cells of the nervous system and the cre-recombinase under the nestin promoter has been used to induce loxP recombination throughout the nervous system early in development (Dubois *et al.* 2006). With the MADM scheme, occasionally cells in the nervous system expressing the nestin driven cre-recombinase will undergo mitotic recombination and functional GFP

and tdTomato sequences are restored during this inter-chromosomal recombination, which are then segregated and expressed in different progeny. The result is the specific labelling of clones of cells expressing GFP (green), or tdTomato (red), or both GFP and tdTomato (yellow), or neither (colourless). Because *mceph* is on the MADM6-TG chromosome and the wild-type gene for Kv1.1 is on the MADM6-GT chromosome, homozygous *mceph*/*mceph* mutant progeny cells are labelled with red colour, homozygous wild-type progeny cells are labelled with green colour and heterozygous *mceph*/+ progeny cells are either yellow or colourless (Fig. 1). Hence, we can identify homozygous *mceph*/*mceph* cells as the red cells for quantitative analyses. The low frequency of recombination events (Zong *et al.* 2005) allows us to characterize the cell-autonomous phenotype of homozygous *mceph*/*mceph* cells surrounded predominantly by phenotypically normal heterozygous cells carrying one *mceph* mutation.

mceph/*mceph* hippocampal neurons are hyperplastic

We began by counting neurons with different colours in the hippocampus from 3-month-old *mceph*-MADM6 mice, at a developmental stage when *mceph*/*mceph* mutant mice have already developed enlarged brains (Donahue *et al.* 1996). In the hippocampus from the nestin-cre;*mceph*-MADM6 mouse, there were two morphologically distinguishable types of cells (Fig. 2*A*): one group of cells have pyramidal or round cell body with thin and elongated processes and most of those cells were immuno-positive for NeuN, a specific marker for neurons (Mullen *et al.* 1992) (Fig. 2*B–D*). The second group of cells have a bushy appearance with diffuse processes, and those cells were positive for GFAP, a specific marker for astrocytes, the predominant glial cells in the hippocampus (Zhou *et al.* 2007) (Fig. 2*F–H*). We counted the number of florescent cells in the hippocampus and identified them as neurons or astrocytes based on their distinct morphology. We next asked if *mceph* induced hyperplasia

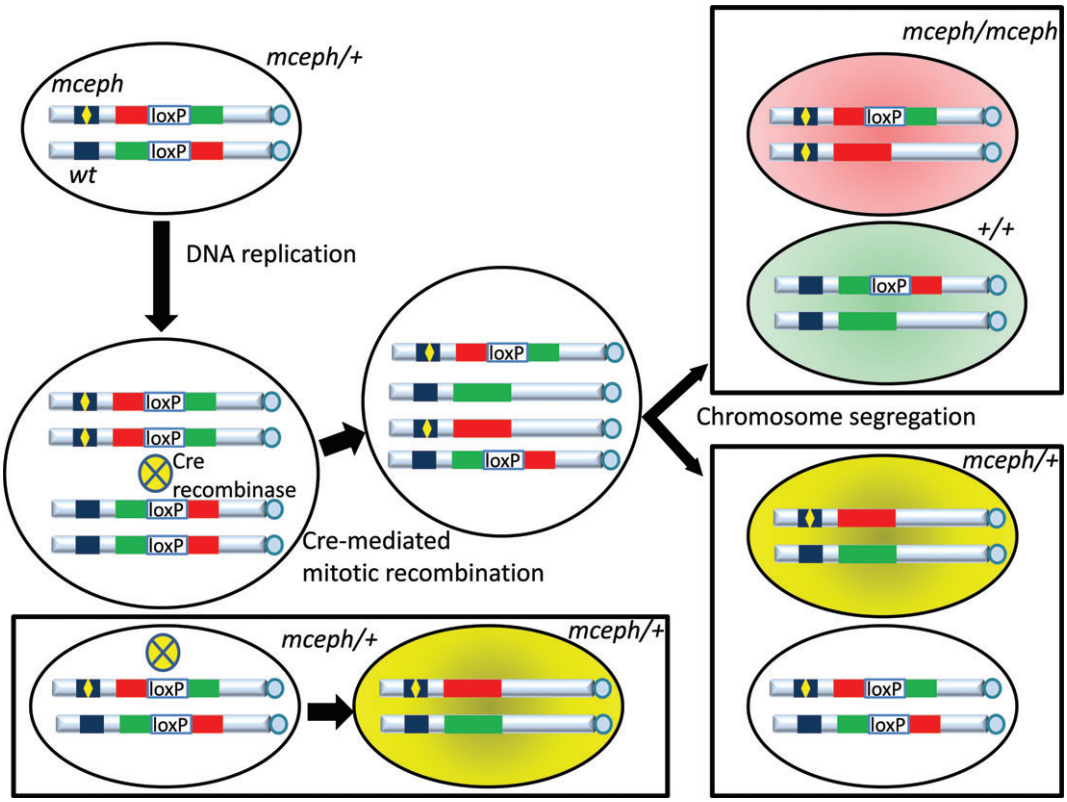

Figure 1. Paradigm for generating the *mceph*-MADM6 mice
MADM6 markers were bred into *mceph*/+ mice, with the *mceph* mutation distal to the MADM6-TG insertion. During S phase, DNA is replicated and, in the presence of cre-recombinase (in this case cre-recombinase expression is controlled under the nestin promoter, which turns on early in neural progenitor cells), infrequent interchromosomal recombination takes place and the functional GFP and tdTomato genes are restored. During chromosome segregation, there will be equal numbers of homozygous *mceph*/*mceph* (red) and wild-type (green) precursor cells, and equal numbers of cells with duo colour (yellow), or colourless, which are heterozygous *mceph*/+. Lower diagram illustrates interchromosomal recombination in the presence of cre-recombinase in non-dividing cells. Recombination happening at this stage will generate more yellow *mceph*/+ cells and hence there are more yellow cells than red and green cells.

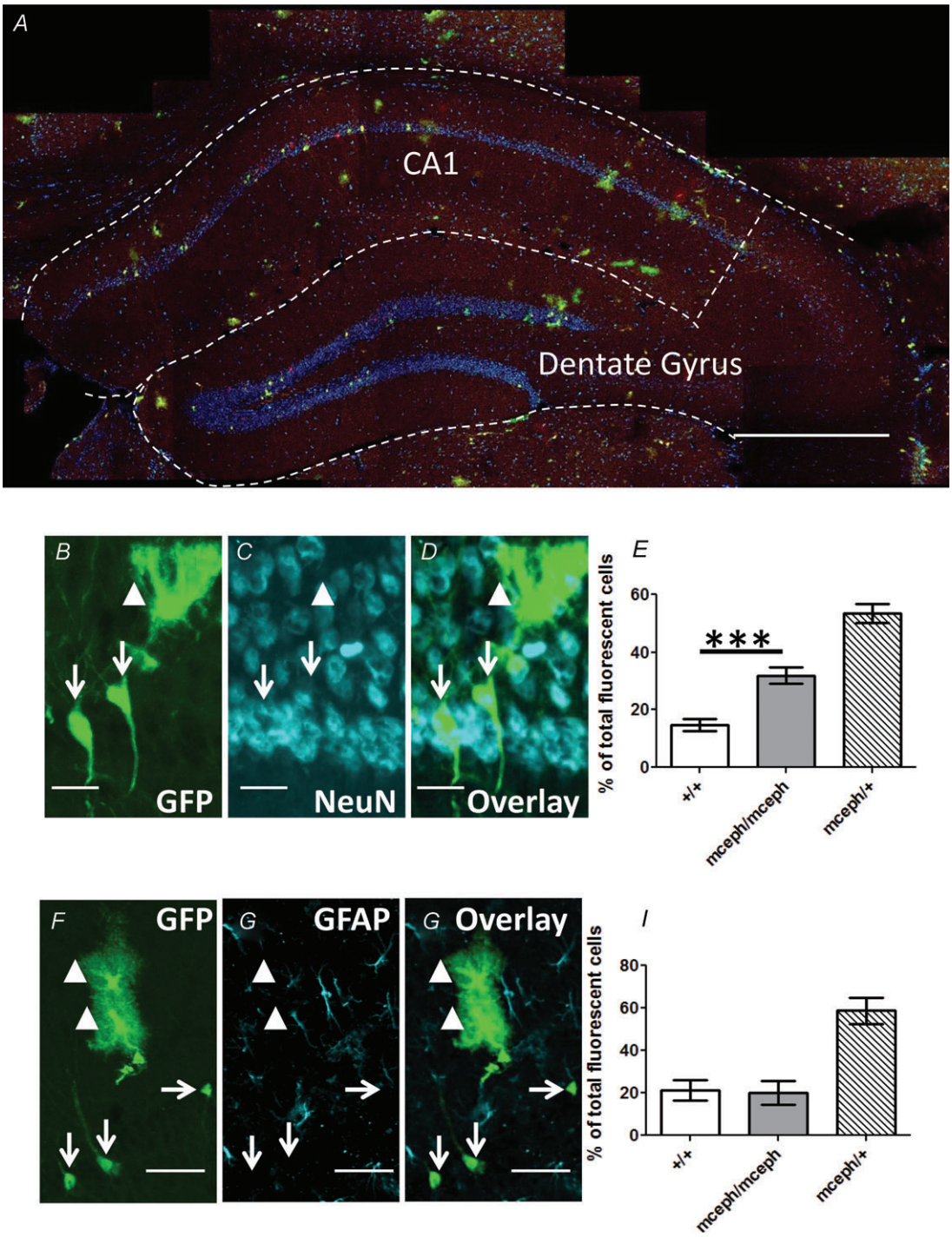

Figure 2. MADM analysis of the *mceph*/+ hippocampus
A, a representative overview image of a hippocampal section from an adult mceph-MADM6 mouse. DAPI counterstain (blue signals) was used for revealing brain structures. Scale bar = 500 μm. *B–D* and *F–H*, cells that have a round or pyramidal cell body and carry distinct thin and long processes are neurons (white arrows), since most of the cells with this type of morphology are positive for NeuN (*C*), a specific marker for neurons, and negative for GFAP (*G*), a specific marker for astrocytes (*D* and *H*); cells that exhibited a bushy appearance (white arrowheads) were negative for NeuN (*C*) but were positive for GFAP (*G*) and therefore those cells with such bushy appearance were defined as astrocytes (*D* and *H*). *E*, statistical analysis of red *mceph*/*mceph* neurons, green wild-type neurons and yellow *mceph*/+ neurons in hippocampus. There were more *mceph*/*mceph* neurons than green wild-type neurons in the hippocampus ($P < 0.001$, Student's *t* test, $n = 47$). *I*, in contrast, there were equal numbers of red *mceph*/*mceph* astrocytes and green wild-type astrocytes in the hippocampus ($P > 0.05$, Student's *t* test, $n = 36$). Scale bar = 20 μm in *B–D* and 40 μm in *F–H*.

is cell-autonomous, since only a very small percentage of the total cell population in *mceph*-MADM6 hippocampus are *mceph*/*mceph* neurons. As we described in the previous section, homozygous *mceph*/*mceph* neurons are labelled with red fluorescence whereas wild-type neurons arising from sibling progenitors that have undergone somatic recombination are green, so we divided the number of red, green and yellow neurons by the total number of fluorescent neurons to determine the respective percentage. We found that in the *mceph*-MADM6 hippocampus there were many more red *mceph*/*mceph* neurons than green wild-type neurons in the hippocampal region (Fig. 2*E*). In contrast, there were comparable numbers of red (*mceph*/*mceph*) and green (wild-type) astrocytes in the *mceph*-MADM6 hippocampus (Fig. 2*I*).

Neurogenesis is known to persist in the hippocampus, especially in the dentate gyrus in adult mammals (Ming & Song, 2005). We next separately analysed the neurons in the CA1 region and dentate gyrus (Fig. 2*A*). We found that in the CA1 region of the hippocampus from the mceph-MADM6 mice there is a slight but significant increase of *mceph*/*mceph* pyramidal neurons (Fig. 3). Moreover, in the dentate gyrus region, the red *mceph*/*mceph* granule cells were dramatically increased as compared to wild-type green cells (Fig. 4). We also have noticed that those red *mceph*/*mceph* granule cells were often clustered and close to one another (Fig. 4*B* and *C*), indicating they may share common ancestry progenitor cells. To control for the possibility that the excessive red neuron counts in *mceph*-MADM6 mice are due to a difference in fluorescent protein expression or detection

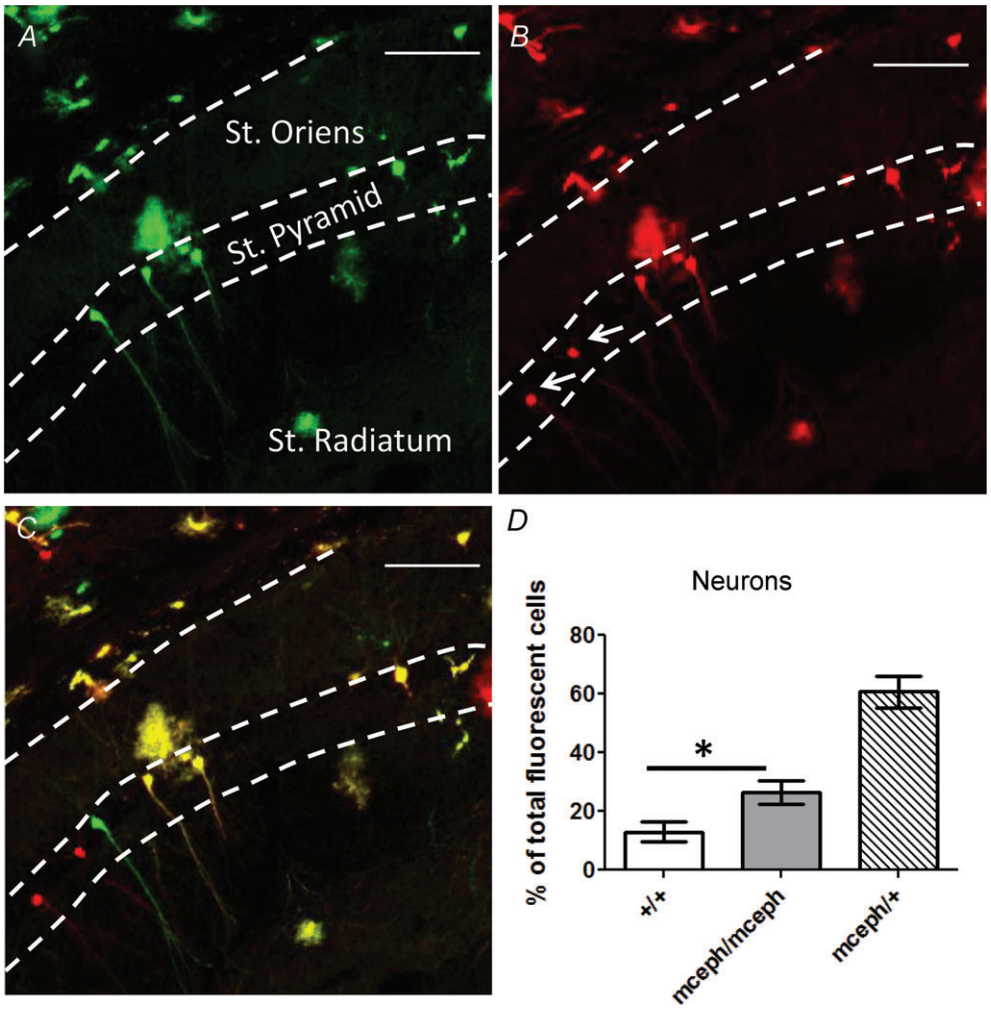

Figure 3. MADM analysis of the CA1 region in the *mceph*-MADM6 hippocampus
A, GFP signals representing the chromosome with the wild-type Kv1.1 gene. *B*, tdTomato signals representing the chromosome with the *mceph* mutation. *C*, overlay of signals in *A* and *B*. *D*, statistical analysis of red neurons, green neurons and yellow neurons in hippocampal CA1 region. There were more red *mceph*/*mceph* neurons than green wild-type neurons in the CA1 hippocampus ($P < 0.05$, Student's *t* test). $n = 14$ for each group. Scale bar = 100 μm.

sensitivity, we also generated wild-type-Kv1.1-MADM6 mice. We found there were equal numbers of red and green neurons in such wild-type hippocampus (Fig. 5), indicating that deleting Kv1.1 is the primary cause of the increase of red *mceph*/*mceph* neurons in *mceph*-MADM6 mice. Meanwhile, we have also noticed that there were more yellow neurons than red and green neurons and this might be caused by cre-mediated recombination in non-dividing neurons (Fig. 1). This phenomenon has been reported previously (Zong *et al.* 2005). Unlike the hippocampus, the size of other parts of the homozygous *mceph*/*mceph* brain seem to be relatively normal (Almgren *et al.* 2007). We asked whether the increase in *mceph*/*mceph* neuron number is restricted to the hippocampus by counting fluorescent neurons in the dorsal cortex (including the entorhinal and parietal cortex), which is adjacent to the hippocampus. We found this part of the cerebral cortex did not exhibit an overgrowth phenotype; in the dorsal cortex there are equal numbers of red *mceph*/*mceph* neurons and green wild-type neurons (Fig. 6).

In addition to hyperplasia, an enlarged brain may also result from hypertrophy such as an increase in the individual cell size. Since we have found that the *mceph*/*mceph* granule cells in the dentate gyrus are the most numerous among the whole hippocampus, indicating the Kv1.1 gene may have greater effect in the granule cells and their progenitors. We measured the soma volume of homozygous, red, *mceph*/*mceph* and heterozygous, yellow, *mceph*/+ neurons, as well as wild-type green granule cells in the dentate gyrus. Similar to the earlier stereological study, although *mceph*/*mceph* granule cells are hyperplastic, we found that those red *mceph*/*mceph* granule cells had comparable soma volume

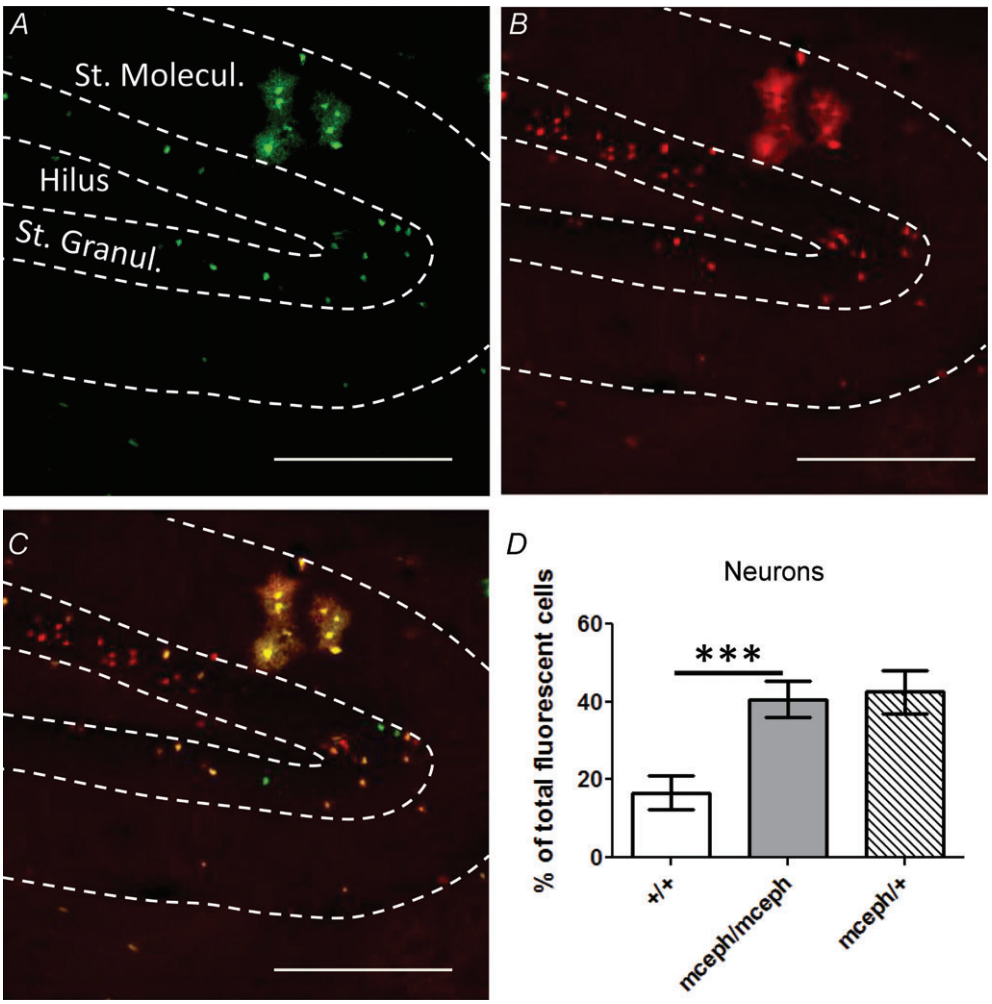

Figure 4. MADM analysis of the dentate gyrus in the *mceph*-MADM6 hippocampus
A, GFP signals representing the chromosome with the wild-type Kv1.1 gene. *B*, tdTomato signals representing the chromosome with the *mceph* mutation. *C*, overlay of signals in *A* and *B*. *D*, statistical analysis of red neurons, green neurons and yellow neurons in hippocampus. There were more red *mceph*/*mceph* neurons than green wild-type neurons in the hippocampus ($P < 0.001$, Student's *t* test). $n = 16$ for each group. Scale bar = 200 μm.

as compared to heterozygous *mceph*/+ and wild-type granule cells in the dentate gyrus (Fig. 7).

Discussion

Using the MADM method for mosaic analysis, we have discovered a cell-autonomous hyperplastic effect of the Kv1.1 mutation in a region-specific and cell type-specific manner, because *mceph*/*mceph* neurons but not *mceph*/*mceph* glial cells in the hippocampus nor *mceph*/*mceph* cortical neurons in the adjacent dorsal cortex (including the entorhinal and parietal cortex) exhibited such an abnormal overgrowth phenotype in adult brains (Figs 2–6). It seems possible that the enlarged brain results from a combination of neural progenitor overproliferaction and a reduction of apoptosis of neurons and possibly their progenitors.

Kv1.1 exhibits an uneven temporal and spatial distribution pattern in the mouse brain. Kv1.1 mRNA has two expression periods during development. The first wave of Kv1.1 expression peaks during embryogenesis around E14.5 and then gradually fades away. The second wave of Kv1.1 mRNA expression peaks around P15 and then maintains a relatively high level throughout adulthood (Hallows & Tempel, 1998; Prüss *et al.* 2010). This tightly regulated temporal expression of Kv1.1 – taken together with our findings – implies an important role of Kv1.1 channel protein in suppressing neurogenesis, since the Kv1.1 mRNA temporal expression pattern coincides with that for neurogenesis: most of the neuronal precursor cells are born between E12 and E19 and the mouse brain reaches its final size around the 3rd week of age (Wullimann, 2009); in between these two time periods the Kv1.1 mRNA expression is relatively low and creates a

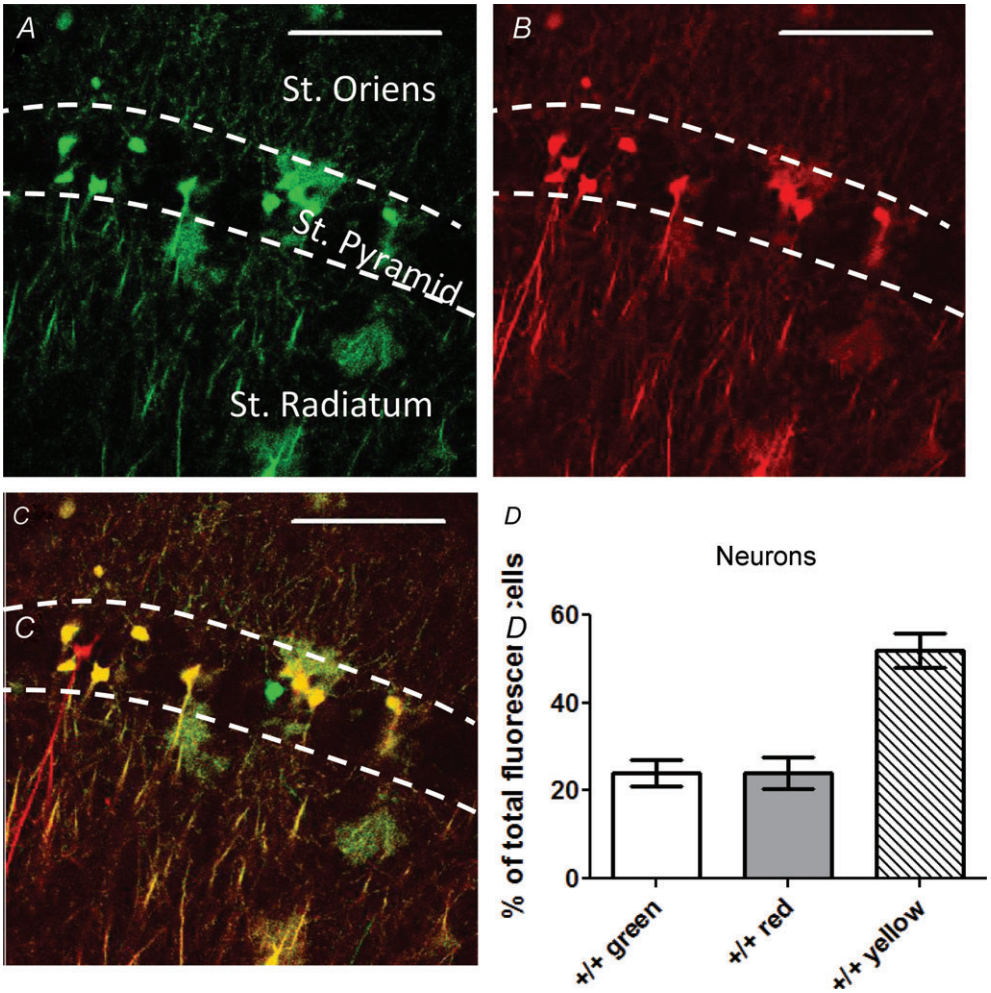

Figure 5. MADM analysis of the wild-type-MADM6 hippocampus
A, GFP signals representing one chromosome 6 with the wild-type Kv1.1 gene. *B*, tdTomato signals representing the other chromosome 6 with the wild-type Kv1.1 gene. *C*, overlay of signals in *A* and *B*. Arrowheads indicate red neurons, arrows indicate green neurons. *D*, statistical analysis of red neurons, green neurons and yellow neurons in hippocampus. There were equal numbers of red and green neurons in the hippocampus ($P > 0.05$, Student's *t* test). $n = 20$ for each group. Scale bar = 100 μm.

time window for neurogenesis. At the adult stage when the Kv1.1 mRNA is at high levels, it is not evenly distributed throughout the brain, but is especially high in the dentate gyrus and the CA2/3 regions in the hippocampus where neurogenesis is known to take place in adulthood (Grosse *et al.* 2000; Prüss *et al.* 2010). As we described earlier, the *mceph* mutation results in a truncated Kv1.1 protein with an intact N-terminal T1 tetramerization domain. This truncated protein does not form a functional Kv channel; rather, since the N-terminal T1 domain is still intact, this truncated Kv1.1 protein could still co-assemble with other α-subunits in the Kv1 family such as Kv1.2 and Kv1.3; *in vitro* heterologous expression study has shown that co-expression of the MCEPH protein in *Xenopus* oocytes suppresses potassium currents mediated by other Kv1 channels (Persson *et al.* 2005). Because the Kv1.1 null mutant mice also exhibit megencephalic phenotype with especially enlarged hippocampus and ventral cortex (Persson *et al.* 2007), this phenotype is likely to be the result of abolished Kv1.1 channel function. It thus appears that Kv1.1-containing channels are important in restricting the neuronal number, since the sparsely generated *mceph*/*mceph* neurons without Kv1.1-containing channels are much more numerous (Figs 2–4).

In *mceph*/*mceph* mice, the enlarged hippocampus also contains an excessive number of astrocytes (Almgren *et al.* 2007). However, in our *mceph*-MADM6 mice, those *mceph*/*mceph* astrocytes did not hold an advantage in cell proliferation and/or survival (Fig. 2). In contrast to its expression in neurons, the Kv1.1 expression level in astrocytes is relatively low (Smart *et al.* 1997; Bekar

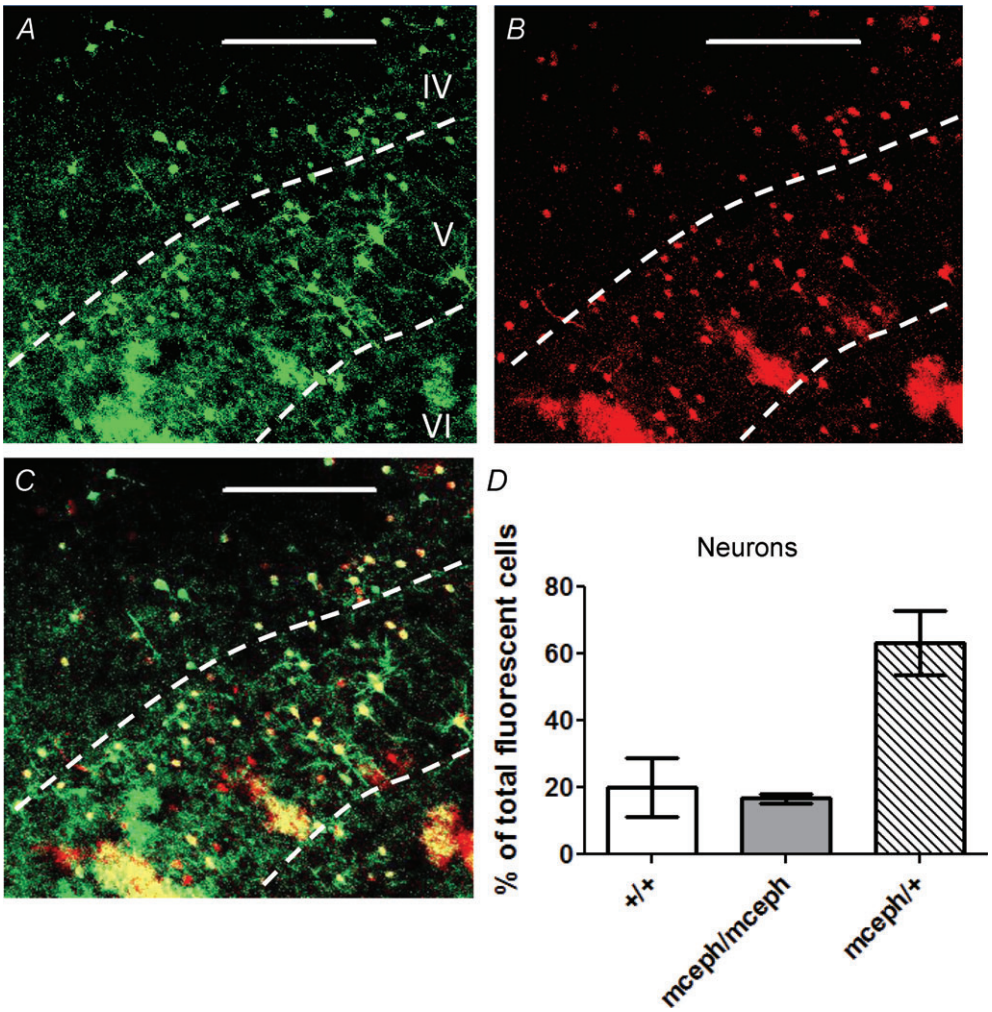

Figure 6. MADM analysis of the *mceph*/+ entorhinal cortex
A, GFP signals representing the chromosome with the wild-type Kv1.1 gene. *B*, tdTomato signals representing the chromosome with the *mceph* mutation. *C*, overlay of signals in *A* and *B*. *D*, statistical analysis of red *mceph*/*mceph* neurons, green wild-type neurons and yellow *mceph*/+ neurons in the entorhinal cortex. There were equal numbers of red *mceph*/*mceph* neurons and green wild-type neurons in the entorhinal cortex ($P > 0.05$, Student's *t* test). $n = 4$ for each group. Scale bar = 200 μm.

et al. 2005; Beraud *et al.* 2006). It has been shown that newborn neurons recruit astrocytes migrating into their newly established territories (Kaneko *et al.* 2010); additionally, increased neuronal activity is also known to stimulate glial cell proliferation (Ongür *et al.* 2007). Moreover, over-reactive astrocytes have been detected at the inferior colliculus and hippocampus in *mceph*/*mceph* mice after acoustic startle stimulation (Fisahn *et al.* 2011). Based on those findings, we hypothesize that the increase of astrocytes observed in *mceph*/*mceph* mice may be caused by non-cell-autonomous mechanisms such as increased astrocyte proliferation induced by hyper-excitable *mceph*/*mceph* neurons with reduced Kv1 channel activity (Smart *et al.* 1998) and/or increased proliferation following hyperplasia of *mceph*/*mceph* neurons to keep neuron-glia ratio constant (Geisert *et al.* 2002).

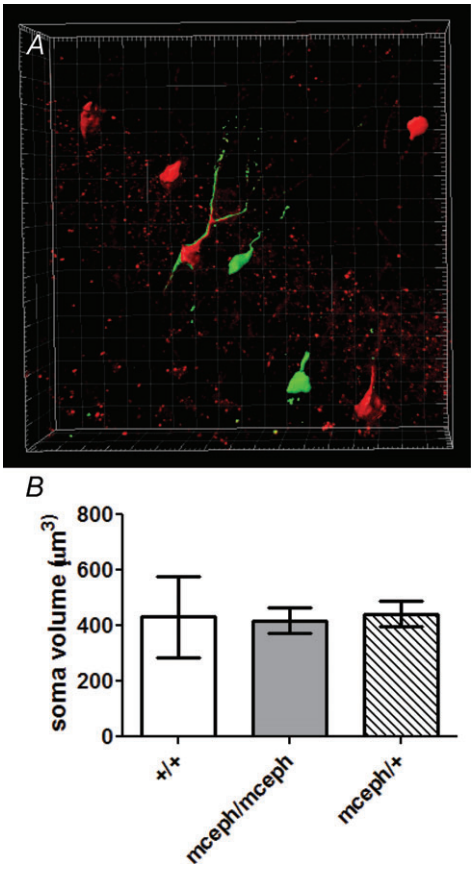

Figure 7. Red *mceph*/*mceph* hippocampal neurons were comparable in size as compared to green wild-type neurons and yellow *mceph*/+ neurons
A, representative 3-demensional reconstruction of granule cells in the dentate gyrus from a *mceph*-MADM6 mouse. *mceph*/*mceph*, wild-type and *mceph*/+ neurons were outlined in red, green and red/green contour, respectively. *B*, statistical analysis of the soma volume from red *mceph*/*mceph* neurons, green wild-type neurons and yellow *mceph*/+ neurons in hippocampus. Red *mceph*/*mceph* neurons had soma size comparable to that of yellow *mceph*/+ neurons and green wild-type neurons in the hippocampus ($P > 0.05$, Student's *t* test). $n = 3$, 13 and 10 for wild-type, *mceph*/*mceph* and *mceph*/+ neurons, respectively. Each grid in *A*represents 10×10 μm.

Potassium channels are important regulators in cell growth and cell proliferation. Altered expression of potassium channels has been found in highly proliferative cells such as cancers and certain potassium channels can control cancer cell proliferation, migration and metastasis (Pardo, 2004). It is well-established that the EAG1 potassium channel is oncogenic, since pharmacological blockade or genetic silencing of EAG1 can effectively reduce tumour size *in vivo* (Pardo *et al.* 1999). As for the Kv1 family, Kv1.3 and Kv1.5 transcripts have been detected at high levels in human cancer biopsies (Bielanska *et al.* 2009). In contrast, our study indicates that Kv1.1 is likely to be anti-proliferative in the progenitors for pyramidal neurons in the CA1 and granule cells in the dentate gyrus of the hippocampus (Figs 2–4), presumably because their precursors without Kv1.1 are more proliferative though it is also possible that without Kv1.1 neurons and/or their precursors refrain from undergoing apoptosis. Kv1.1-containing channels operate at more negative membrane potential than most other potassium channels; in addition, these channels inactivate much more slowly than other channels in the Kv1 family (Storm, 1988). Whether and how Kv1.1 suppresses neurogenesis in the hippocampus is currently unknown. Based on the unique biophysical property of Kv1.1, it is conceivable that hippocampal neural progenitors without Kv1.1-containing channels are more excitable and hyper-excitability may increase intracellular calcium, a vital intracellular ion to trigger cell proliferation (Apáti *et al.* 2011). Moreover, removal of Kv1.1 may cause a reduction in the intracellular potassium loss, which has the potential to promote cell survival and avert the initiation of the cell signalling cascade that leads to apoptosis (Bortner & Cidlowski, 2007). Indeed, homozygous *mceph*/*mceph* mice have a reduced apoptotic rate in the hippocampus (Almgren *et al.* 2007, 2008). Along the same line, an astrocyte specific sodium channel has been shown to control the viability of astrocytes in the spinal cord independent of the electrogenic role of sodium channels. Sontheimer and colleagues (1994) demonstrated that this astrocyte specific sodium channel controls intracellular sodium concentration, which leads to the activation of the Na^+,K^+-ATPase. Blocking this sodium channel by tetrodotoxin causes a depletion of intracellular sodium, slows down the Na^+,K^+-ATPase, and, as a consequence, results in excessive depolarization and massive calcium influx which may lead to cell death and apoptosis. It will be important to pursue further studies such as double labelling with TUNEL and BrdU at the subventricular zone (Ming & Song, 2005) or the subgranular zone in the dentate gyrus (Li & Pleasure, 2007), two regions with robust adult neurogenesis, in *mceph*-MADM6 mice.

Extending studies such as the MADM analysis to mice of older ages will also be informative in assessing the relative contribution of reduced apoptosis and increased proliferation to the ever growing brain of *mceph* mutant mice.

In summary, using the innovative technology provided by the MADM mice, we have revealed a novel cell-autonomous function of Kv1.1 in the control of neuron numbers, thereby attributing Kv1 channel functions beyond what Hodgkin and Huxley proposed for hyperpolarization and repolarization of the action potential. It seems likely that there are other unexpected functions of potassium channels waiting to be discovered in the future.

References

Almgren M, Nyengaard JR, Persson B & Lavebratt C (2008). Carbamazepine protects against neuronal hyperplasia and abnormal gene expression in the megencephaly mouse. *Neurobiol Dis* **32**, 364–376.

Almgren M, Persson AS, Fenghua C, Witgen BM, Schalling M, Nyengaard JR & Lavebratt C (2007). Lack of potassium channel induces proliferation and survival causing increased neurogenesis and two-fold hippocampus enlargement. *Hippocampus* **17**, 292–304.

Apáti A, Pászty K, Erdei Z, Szebényi K, Homolya L & Sarkadi B (2011). Calcium signaling in pluripotent stem cells. *Mol Cell Endocrinol* **353**, 57–67.

Bekar LK, Loewen ME, Cao K, Sun X, Leis J, Wang R, Forsyth GW & Walz W (2005). Complex expression and localization of inactivating Kv channels in cultured hippocampal astrocytes. *J Neurophysiol* **93**, 1699–1709.

Beraud E, Viola A, Regaya I, Confort-Gouny S, Siaud P, Ibarrola D, Le Fur Y, Barbaria J, Pellissier JF, Sabatier JM, Medina I & Cozzone PJ (2006). Block of neural Kv1.1 potassium channels for neuroinflammatory disease therapy. *Ann Neurol* **60**, 586–596.

Bernstein J (1902). Untersuchungen zur Thermodynamik der bioelektrischen Ströme Erster Theil. *Pflügers Archiv*, **92**, 521–562.

Bielanska J, Hernández-Losa J, Pérez-Verdaguer M, Moline T, Somoza R, Ramón Y Cajal S, Condom E, Ferreres JC & Felipe A (2009). Voltage-dependent potassium channels Kv1.3 and Kv1.5 in human cancer. *Curr Cancer Drug Targets* **9**, 904–914.

Bortner CD & Cidlowski JA (2007). Cell Shrinkage and monovalent cation fluxes: role on apoposis. *Arch biochem Biophys* **462**(2), 176–188.

Campomanes CR, Carroll KI, Manganas LN, Hershberger ME, Gong B, Antonucci DE, Rhodes KJ & Trimmer JS (2002). Kv beta subunit oxidoreductase activity and Kv1 potassium channel trafficking. *J Biol Chem* **277**, 8298–8305.

Covarrubias M, Wei AA & Salkoff L (1991). Shaker, Shal, Shab, and Shaw express independent K^+ current systems. *Neuron* **7**, 763–773.

Diez M, Schweinhardt P, Petersson S, Wang FH, Lavebratt C, Schalling M, Hökfelt T & Spenger C (2003). MRI and in situ hybridization reveal early disturbances in brain size and gene expression in the megencephalic (mceph/mceph) mouse. *Eur J Neurosci* **18**, 3218–3230.

Donahue LR, Cook SA, Johnson KR, Bronson RT & Davisson MT (1996). Megencephaly: a new mouse mutation on chromosome 6 that causes hypertrophy of the brain. *Mamm Genome* **7**, 871–876.

Dubois NC, Hofmann D, Kaloulis K, Bishop JM & Trumpp A (2006). Nestin-Cre transgenic mouse line Nes-Cre1 mediates highly efficient Cre/loxP mediated recombination in the nervous system, kidney, and somite-derived tissues. *Genesis* **44**, 355–360.

Espinosa JS, Wheeler DG, Tsien RW & Luo L (2009). Uncoupling dendrite growth and patterning: single-cell knockout analysis of NMDA receptor 2B. *Neuron* **62**, 205–217.

Fisahn A, Lavebratt C & Canlon B (2011). Acoustic startle hypersensitivity in Mceph mice and its effect on hippocampal excitability. *Eur J Neurosci* **34**, 1121–1130.

Geisert EE, Williams RW, Geisert GR, Fan L, Asbury AM, Maecker HT, Deng J & Levy S (2002). Increased brain size and glial cell number in CD81-null mice. *J Comp Neurol* **453**, 22–32.

Glazebrook PA, Ramirez AN, Schild JH, Shieh CC, Doan T, Wible BA & Kunze DL (2002). Potassium channels Kv1.1, Kv1.2 and Kv1.6 influence excitability of rat visceral sensory neurons. *J Physiol* **541**, 467–482.

Grosse G, Draguhn A, Höhne L, Tapp R, Veh RW & Ahnert-Hilger G (2000). Expression of Kv1 potassium channels in mouse hippocampal primary cultures: development and activity-dependent regulation. *J Neurosci* **20**, 1869–1882.

Guan D, Lee JC, Tkatch T, Surmeier DJ, Armstrong WE & Foehring RC (2006). Expression and biophysical properties of Kv1 channels in supragranular neocortical pyramidal neurones. *J Physiol* **571**, 371–389.

Gutman GA, Chandy KG, Grissmer S, Lazdunski M, McKinnon D, Pardo LA, Robertson GA, Rudy B, Sanguinetti MC, Stühmer W & Wang X (2005). International Union of Pharmacology. LIII. Nomenclature and molecular relationships of voltage-gated potassium channels. *Pharmacol Rev* **57**, 473–508.

Hallows JL & Tempel BL (1998). Expression of Kv1.1, a Shaker-like potassium channel, is temporally regulated in embryonic neurons and glia. *J Neurosci* **18**, 5682–5691.

Heeroma JH, Henneberger C, Rajakulendran S, Hanna MG, Schorge S & Kullmann DM (2009). Episodic ataxia type 1 mutations differentially affect neuronal excitability and transmitter release. *Dis Model Mech* **2**, 612–619.

Herrero-Herranz E, Pardo LA, Bunt G, Gold R, Stühmer W & Linker RA (2007). Re-expression of a developmentally restricted potassium channel in autoimmune demyelination: Kv1.4 is implicated in oligodendroglial proliferation. *Am J Pathol* **171**, 589–598.

Hodgkin AL & Huxley AF (1952*a*). A quantitative description of membrane current and its application to conduction and excitation in nerve. *J Physiol* **117**, 500–544.

Hodgkin AL & Huxley AF (1952*b*). The components of membrane conductance in the giant axon of *Loligo*. *J Physiol* **116**, 473–496.

Jan LY & Jan YN (1997). Voltage-gated and inwardly rectifying potassium channels. *J Physiol* **505**, 267–282.

Kaneko N, Marín O, Koike M, Hirota Y, Uchiyama Y, Wu JY, Lu Q, Tessier-Lavigne M, Alvarez-Buylla A, Okano H, Rubenstein JL & Sawamoto K (2010). New neurons clear the path of astrocytic processes for their rapid migration in the adult brain. *Neuron* **67**, 213–223.

Lavebratt C, Trifunovski A, Persson AS, Wang FH, Klason T, Ohman I, Josephsson A, Olson L, Spenger C & Schalling M (2006). Carbamazepine protects against megencephaly and abnormal expression of BDNF and Nogo signaling components in the mceph/mceph mouse. *Neurobiol Dis* **24**, 374–383.

Li G & Pleasure SJ (2007). Genetic regulation of dentate gyrus morphogenesis. *Prog Brain Res* **163**, 143–152.

Li M, Jan YN & Jan LY (1992). Specification of subunit assembly by the hydrophilic amino-terminal domain of the Shaker potassium channel. *Science* **257**, 1225–1230.

Liu C, Sage JC, Miller MR, Verhaak RG, Hippenmeyer S, Vogel H, Foreman O, Bronson RT, Nishiyama A, Luo L & Zong H (2011). Mosaic analysis with double markers reveals tumor cell of origin in glioma. *Cell* **146**, 209–221.

Long SB, Tao X, Campbell EB & MacKinnon R (2007). Atomic structure of a voltage-dependent K^+ channel in a lipid membrane-like environment. *Nature* **450**, 376–382.

Ming GL & Song H (2005). Adult neurogenesis in the mammalian central nervous system. *Annu Rev Neurosci* **28**, 223–250.

Mullen RJ, Buck CR & Smith AM (1992). NeuN, a neuronal specific nuclear protein in vertebrates. *Development* **116**, 201–211.

Ongür D, Pohlman J, Dow AL, Eisch AJ, Edwin F, Heckers S, Cohen BM, Patel TB & Carlezon WA (2007). Electroconvulsive seizures stimulate glial proliferation and reduce expression of Sprouty2 within the prefrontal cortex of rats. *Biol Psychiatry* **62**, 505–512.

Papazian DM, Schwarz TL, Tempel BL, Jan YN & Jan LY (1987). Cloning of genomic and complementary DNA from Shaker, a putative potassium channel gene from *Drosophila*. *Science* **237**, 749–753.

Pardo LA (2004). Voltage-gated potassium channels in cell proliferation. *Physiology (Bethesda)* **19**, 285–292.

Pardo LA, del Camino D, Sánchez A, Alves F, Brüggemann A, Beckh S & Stühmer W (1999). Oncogenic potential of EAG K^+ channels. *EMBO J* **18**, 5540–5547.

Persson AS, Klement G, Almgren M, Sahlholm K, Nilsson J, Petersson S, Arhem P, Schalling M & Lavebratt C (2005). A truncated Kv1.1 protein in the brain of the megencephaly mouse: expression and interaction. *BMC Neurosci* **6**, 65.

Persson AS, Westman E, Wang FH, Khan FH, Spenger C & Lavebratt C (2007). Kv1.1 null mice have enlarged hippocampus and ventral cortex. *BMC Neurosci* **8**, 10.

Petersson S, Persson AS, Johansen JE, Ingvar M, Nilsson J, Klement G, Arhem P, Schalling M & Lavebratt C (2003). Truncation of the Shaker-like voltage-gated potassium channel, Kv1.1, causes megencephaly. *Eur J Neurosci* **18**, 3231–3240.

Preussat K, Beetz C, Schrey M, Kraft R, Wölfl S, Kalff R & Patt S (2003). Expression of voltage-gated potassium channels Kv1.3 and Kv1.5 in human gliomas. *Neurosci Lett* **346**, 33–36.

Prüss H, Grosse G, Brunk I, Veh RW & Ahnert-Hilger G (2010). Age-dependent axonal expression of potassium channel proteins during development in mouse hippocampus. *Histochem Cell Biol* **133**, 301–312.

Shen W, Hernandez-Lopez S, Tkatch T, Held JE & Surmeier DJ (2004). Kv1.2-containing K^+ channels regulate subthreshold excitability of striatal medium spiny neurons. *J Neurophysiol* **91**, 1337–1349.

Sheng M, Tsaur ML, Jan YN & Jan LY (1992). Subcellular segregation of two A-type K^+ channel proteins in rat central neurons. *Neuron* **9**, 271–284.

Shieh CC, Coghlan M, Sullivan JP & Gopalakrishnan M (2000). Potassium channels: molecular defects, diseases, and therapeutic opportunities. *Pharmacol Rev* **52**, 557–594.

Smart SL, Bosma MM & Tempel BL (1997). Identification of the delayed rectifier potassium channel, Kv1.6, in cultured astrocytes. *Glia* **20**, 127–134.

Smart SL, Lopantsev V, Zhang CL, Robbins CA, Wang H, Chiu SY, Schwartzkroin PA, Messing A & Tempel BL (1998). Deletion of the $K_V1.1$ potassium channel causes epilepsy in mice. *Neuron* **20**, 809–819.

Sontheimer H, Fernandez-Marques E, Ullrich N, Pappas CA & Waxman SG (1994). Astrocyte Na^+ channels are required for maintenance of Na^+/K^+-ATPase activity. *J Neurosci* **14**, 2464–2475.

Storm JF (1988). Temporal integration by a slowly inactivating K^+ current in hippocampal neurons. *Nature* **336**, 379–381.

Stühmer W, Ruppersberg JP, Schröter KH, Sakmann B, Stocker M, Giese KP, Perschke A, Baumann A & Pongs O (1989). Molecular basis of functional diversity of voltage-gated potassium channels in mammalian brain. *EMBO J* **8**, 3235–3244.

Wang H, Kunkel DD, Schwartzkroin PA & Tempel BL (1994). Localization of Kv1.1 and Kv1.2, two K channel proteins, to synaptic terminals, somata, and dendrites in the mouse brain. *J Neurosci* **14**, 4588–4599.

Wonderlin WF & Strobl JS (1996). Potassium channels, proliferation and G1 progression. *J Membr Biol* **154**, 91–107.

Wullimann MF (2009). Secondary neurogenesis and telencephalic organization in zebrafish and mice: a brief review. *Integr Zool* **4**, 123–133.

Zhou W, Ge WP, Zeng S, Duan S & Luo Q (2007). Identification and two-photon imaging of oligodendrocyte in CA1 region of hippocampal slices. *Biochem Biophys Res Commun* **352**, 598–602.

Zhou Y & MacKinnon R (2003). The occupancy of ions in the K^+ selectivity filter: charge balance and coupling of ion binding to a protein conformational change underlie high conduction rates. *J Mol Biol* **333**, 965–975.

Zong H, Espinosa JS, Su HH, Muzumdar MD & Luo L (2005). Mosaic analysis with double markers in mice. *Cell* **121**, 479–492.

Author contributions

S.B.Y. and K.D.M. performed experiments and data analysis. B.T and L.L. provided experimental materials. S.B.Y., Y.N.J. and L.Y.J. prepared the manuscript. All authors have reviewed and edited the manuscript.

Acknowledgements

We thank Drs Woo-Ping Ge, An-Chi Tien, Jamsine Chen and Grant Li at UCSF for discussions and Dr Hui Zong (Institute of Molecular Biology, University of Oregon, Eugene) for assistance in producing the MADM6 mice. This work was supported by American Diabetes Association Mentor-Based Fellowship 7-06-MN-29 (to S.B.Y.), HHMI Summer Student Program (to K.D.M.), NIH grant R01-NS050835 (to L.L.) and NIMH grant MH065334 (to L.Y.J.). L.L, Y.N.J. and L.Y.J. are investigators of the Howard Hughes Medical Institute.